



Antibiotic-loaded nanoparticles for the treatment of intracellular methicillin-resistant *Staphylococcus Aureus* infections: *In vitro* and *in vivo* efficacy of a novel antibiotic

Gabriella Costabile^{a,b,1}, Domizia Baldassi^{a,1}, Christoph Müller^c, Birgit Groß^d, Francesca Ungaro^b, Sören Schubert^d, Steven M. Firestone^e, Olivia M. Merkel^{a,*}

^a Department of Pharmacy, Pharmaceutical Technology & Biopharmaceutics, Ludwig-Maximilians-Universität München, Butenandstr. 5-13, 81377 Munich, DE, Germany

^b Department of Pharmacy, University of Napoli Federico II, Via Domenico Montesano 49, 80131 Napoli, IT, Italy

^c Department of Pharmacy, Center for Drug Research, Ludwig-Maximilians-Universität München, Butenandstr. 5-13, 81377 Munich, DE, Germany

^d Max von Pettenkofer-Institut Munich für Hygiene und Medizinische Mikrobiologie, Elisabeth-Winterhalter-Weg 6, 81377 Munich, DE, Germany

^e Department of Pharmaceutical Sciences, Eugene Applebaum College of Pharmacy and Health Sciences, Wayne State University, Eugene Applebaum College of Pharmacy and Health Sciences, 259 Mack Ave, Detroit, MI 48201, USA

ARTICLE INFO

Keywords:

PLGA nanoparticles
Benzophenone antibiotics
Sustained release
G. mellonella
Intracellular infections

ABSTRACT

Antimicrobial resistance is considered one of the biggest threats to public health worldwide. Methicillin-resistant *S. aureus* is the causative agent of a number of infections and lung colonization in people suffering from cystic fibrosis. Moreover, a growing body of evidence links the microbiome to the development of cancer, as well as to the success of the treatment. In this view, the development of novel antibiotics is of critical importance, and SV7, a novel antibiotic active against MRSA at low concentrations, represents a promising candidate. However, the low aqueous solubility of SV7 hampers its therapeutic translation. In this study, SV7 was encapsulated in poly (lactic-co-glycolic acid) (PLGA) nanoparticles (NPs) to improve the solubility profile, to ensure sustained release and eventually support deposition in the airways. Furthermore, PLGA NPs were formulated as dry powder to extend their shelf-life and were shown to efficiently target intracellular infections. After identifying a formulation with suitable physico-chemical characteristics, SV7-loaded NPs were investigated *in vitro* in terms of inhibitory activity against MRSA, and their safety profile in lung epithelial cells. Subsequently, the activity against MRSA intracellular infections was investigated in a co-culture model of MRSA and macrophages. To test the translatability of our findings, SV7-loaded NPs were tested *in vivo* in a *Galleria mellonella* infection model. In conclusion, SV7-loaded NPs showed a safe profile and efficient inhibitory activity against MRSA at low concentrations. Furthermore, their activity against intracellular infections was confirmed, and was retained *in vivo*, rendering them a promising candidate for treatment of MRSA lung infections.

1. Introduction

Staphylococcus aureus and its methicillin-resistant phenotype (MRSA) are the causative agents of a wide variety of infections, including endocarditis, osteomyelitis, necrotizing pneumonia, and septic shock [1]. Notably, pulmonary infections triggered by *S. aureus* are associated with a very high case fatality rate and are a leading cause of nosocomial pneumonia and secondary bacterial pneumonia following influenza A

virus infection. Moreover, in a period in which the Human Microbiome Project is gradually unveiling the importance played by the lung microbiome in the diagnosis, progression, and prognosis of other disease, such as lung cancer and cystic fibrosis (CF), MRSA represents a very harmful pathogen in the broader sense [2]. In fact, it has been demonstrated that *S. aureus* is one of the first bacteria able to colonize the airways of CF patients. Here, *S. aureus* produces the conditions for additional infections for example by *Pseudomonas aeruginosa*, which

* Corresponding author at: Department of Pharmacy, Pharmaceutical Technology & Biopharmaceutics, Ludwig-Maximilian University of Munich, Butenandstr. 5-13, 81377 Munich, DE, Germany.

E-mail address: olivia.merkel@lmu.de (O.M. Merkel).

¹ These authors contributed equally.

<https://doi.org/10.1016/j.jconrel.2024.08.029>

Received 19 March 2024; Received in revised form 29 July 2024; Accepted 19 August 2024

Available online 26 August 2024

0168-3659/© 2024 The Authors. Published by Elsevier B.V. This is an open access article under the CC BY-NC-ND license (<http://creativecommons.org/licenses/by-nc-nd/4.0/>).

dramatically worsen the clinical outcome and result in an increased rate of lung function decline [3]. Likewise, recent research starting in 2022 shows a link between the lung microbiome and cancer. The lung microbiome composition varies between stages and the presence of Staphylococci appears abundant in cancer patients, in contrast with noncancerous subjects. This has also been confirmed by the analysis of The Cancer Genome Atlas (TCGA) lung adenocarcinoma and lung squamous cell carcinoma databases [4–6]. Furthermore, it has been shown that defects in the tumor-associated barrier and obstruction of the airways results in impaired bacterial clearance and altered bacteria growth conditions, triggering a strong response of pro-inflammatory mediators and promoting neutrophil expansion. This leads to the establishment of a vicious cycle that exacerbates tumor growth [5]. Thus, even if the connection between the microbiome and the tumor growth is not fully understood yet, pulmonary microorganisms and their products affect clinical treatments, and further investigation is required to find out how to exploit the therapeutic potential behind the use of antibiotics in cancer therapy. Work lead by Prof. Leaf Huang has in fact shown how liposomes, designed to entrap an antibiotic (*i.e.* a silver-tinidazole complex), enabled >70% long-term survival in two *F. nucleatum*-infected colorectal *in vivo* cancer models, while at the same time eliciting anti-tumoral immunity [7].

The clinical management of *S. aureus* lung infections is complicated by the widespread antibiotic resistance present in this bacterium, and its ability to establish intracellular infection within a variety of cell types, including epithelial cells, macrophages, and neutrophils. Accordingly, MRSA escape the immune response, thus causing particular challenges in the treatment of the infection. Once internalized, the pathogen will be protected up to 4–7 days without affecting the host cell viability [8–10].

Currently, the sole treatment option is the use of antibiotics, but with the escalating antimicrobial resistance crisis, treatment failures are on the rise, with a mortality rate of 10–30% [11]. To bolster the fight against MRSA infections and achieve early eradication, prioritizing the development of new antibiotics capable of targeting the bacteria following intracellular infection is crucial. This urgency has been highlighted by the World Health Organization, which has included MRSA in the global priority list of antibiotic-resistant bacteria due to the high mortality and morbidity linked to invasive infections (WHO/EMP/IAU/2017.12).

In this work, we enable a novel active compound, namely SV7, to exert its antimicrobial activity against MRSA despite its strongly hydrophobic nature, and further assessed its efficacy *in vitro* and *in vivo* against intracellular infection of MRSA. SV7 was discovered by Firestine and co-workers, and has shown very promising activity not only against methicillin-sensitive *S. aureus* (MSSA), but also against MRSA strains without inducing antimicrobial resistance (AMR) phenomena. [12,13]. This compound is a novel benzophenone-based membrane-targeting antibiotic that has similarities to the structure and function of antimicrobial peptides (AMPs) and synthetic ion channels [12–14]. SV7 safety of use as well as the ability of curing mice of a lethal MRSA infection has been already shown [13]. However, from a technical standpoint, the major obstacles to SV7 translation into the clinics is its very low aqueous solubility, which can affect its dissolution in physiological fluids. Moreover, it is completely ineffective against intracellular infections since, similar to many other conventional antimicrobials, it shows restricted intracellular penetration and low retention.

In order to overcome these limitations, we propose PLGA-based nanoparticles as a delivery system that could serve the dual purpose of increasing SV7 bioavailability, and help the delivery of SV7 inside host cells to treat the intracellular infections [15–18]. The design and development of SV7-loaded PLGA NPs is presented. The NPs were produced through a single evaporation emulsification method, and the composition was optimized based on size, polydispersity index, surface charge and especially optimum SV7 loading. Considering the major localization of MRSA in the respiratory tract, we have designed the nanoparticle platform towards a possible local application of the SV7-

loaded PLGA NPs *via* inhalation [19]. In fact, by targeting the lungs directly for therapeutic treatment by inhalation, the SV7-loaded particles are able to largely avoid systemic circulation and consequently reduce the patients' exposure to antibiotics, thereby delaying the eventual development of AMR [20]. Additionally, with a sustained release of the drug, a reduced number of administrations can be expected, thus increasing patient adherence to complex therapeutic regimens required for the management of chronic lung diseases [21]. This aspect is particularly welcome for antibiotics therapy, considering the direct correlation between the onset of AMR phenomena and the drug dose [22]. Thus, only the formulation characterized by desirable physicochemical parameters for pulmonary administration were selected [19], and nanoparticles were characterized for morphology, residual content of organic solvents and stability over time. Formulations were further evaluated for the possibility to extend their shelf-life through freeze-drying. To evaluate how the manufacturing process could alter the SV7 release in a physiological environment, the antimicrobial activity and potential cytotoxic effects were tested *in vitro* in suitable models. Furthermore, the potential of the NPs for treating intracellular infections was evaluated in terms of both nanoparticle cellular uptake, as well as activity against MRSA intracellular infection in the J774A.1 macrophage cell line in presence of fluorescently labeled NPs and SV7-loaded NPs, respectively. Finally, activity data on the *in vivo* performance were collected in a *Galleria mellonella* infection model, a valid tool for studying the antimicrobial activity of antibiotics encapsulated in polymeric nanoparticles [23,24], to better support further translation into the clinic. Overall, the preclinical evaluation conducted on the developed SV7-loaded PLGA demonstrate, first *in vitro* and then *in vivo*, the high potential of SV7 in the treatment of infections sustained by MSSA and MRSA strains, even when established intracellularly.

2. Experimental methods

2.1. Materials

SV7 was synthesized as described previously [12,13]. Resomer® RG 502H, Poly(D,L-lactide-co-glycolide) (PLGA) 50:50 (molecular weight (Mw) 7 kDa) was purchased from Evonik Nutrition & Care GmbH (Essen, Germany). Polyvinyl alcohol (PVA) (Mw ~205 kDa), mannitol, trehalose, 2-hydroxypropyl- β -cyclodextrin (HP- β -CD), acetone, and dichloromethane were purchased from Sigma-Aldrich (St Louis, MO, USA). All solvents used were ACS grade solvents.

Human lung adenocarcinoma epithelial cells (A549) and mouse BALB/c monocyte macrophages (J774A.1) were obtained from ATCC (LGC Standards GmbH, Wesel, Germany). The human bronchial epithelial cell line (16HBE14o-) was a kind gift from the Comprehensive Pneumology Center of Munich. Minimum Essential Medium (MEM), Roswell Park Memorial Institute (RPMI) 1640 Medium, Dulbecco's Modified Eagle Medium (DMEM), fetal bovine serum (FBS), L-glutamine, MEM non-essential amino acid solution and penicillin-streptomycin (P/S) for cell culture were purchased from Sigma-Aldrich (St Louis, MO, USA). 3-(4,5-dimethylthiazol-2-yl)-2,5-diphenyltetrazolium bromide (MTT), Lysotracker™ red and trypsin 0.25% (m/v), EDTA were purchased from ThermoFisher Scientific (Waltham, MA, USA). All other chemicals were standard chemicals required for cell and bacterial culture.

Microscope slides were purchased from VWR (Radnor, PA, USA). FluorSave™ reagent was purchased from Merck Millipore (Burlington, MA, USA). 13 mm Karl Hecht™ Assistant™ Circular Cover Glasses for microscopy were purchased from Fischer Scientific (Hampton, NH, USA).

2.2. SV7 analytical quantification

The analytical determination of SV7 was carried out by reverse-phase High-Performance Liquid Chromatography (RP-HPLC) and UV

– vis spectrophotometry. For the determination through RP-HPLC an Agilent 1100/1200 series (Agilent Technologies, USA) equipped with a Synergi™ polar RP column (50 × 2.0 mm, 80 Å) (Phenomenex, USA) was employed. Separation required a gradient elution using 0.2% formic acid in water and 0.2% formic acid in acetonitrile. The gradient was applied as follows: $t = 0$ 10% organic phase (B) ramp to 65% B over 2.5 min. After run, ramp back to 10% B. The flow rate was 1 mL/min and the detection wavelength 265 nm. Under these conditions the retention time of SV7 was 3 min.

The determination through UV spectroscopy was carried out at 265 nm using a microplate reader equipped with a 96 well plate (FLUOstar Omega, BMG Labtech, Ortenberg, Germany) as previously reported [25]. Briefly, a known amount of SV7 was placed into microcentrifuge tubes, then 500 μ L of dichloromethane (DCM) and 1 mL 50 mmol HCl were added. The samples were vortexed, and the two phases were left to separate. Protonated SV7 is present in the aqueous phase. A calibration curve was obtained by plotting absorbance versus the concentration of SV7 standard solutions prepared in DCM. The linearity of the response was verified over a concentration range of 0.5–25 μ g/mL ($r^2 = 0.999$). The extinction coefficient determined from the standard curve was 0.050.

2.3. Production of SV7-loaded PLGA nanoparticles

PLGA nanoparticles as well as SV7-loaded PLGA NPs (PLGA_SV7) were prepared through a single evaporation emulsification method, adapting a protocol previously published [25]. Briefly, the organic phase was prepared by dissolving PLGA in acetone. When needed, SV7 was added to the organic phase. Subsequently, the organic solution was added dropwise to the aqueous phase of PVA (1.0, 1.5 and 2.0% w/v) under magnetic stirring (1200 rpm). The emulsion formed was treated for 10 min with an ultrasound probe sonicator (heat flux density 8.5 W/cm²) and left stirring overnight to evaporate the organic solvent. Nanoparticles were recovered and washed with Milli-Q water by centrifugation at 16,900 \times g and 4 °C for 30 min, the supernatant was discarded, and the entire procedure was repeated twice. The NPs were then suspended in 10 mL of Milli-Q water.

Fluorescently labeled nanoparticles were prepared similarly, but in this case, 10 μ L of coumarin-6 from a stock solution of 50 mg/mL were added to the organic phase containing SV7 and emulsified with 1.5% PVA.

2.4. Characterization of SV7-loaded PLGA nanoparticles

2.4.1. Nanoparticle size, polydispersity index, surface charge

The hydrodynamic diameter (D_H), the polydispersity index (PDI), and zeta potential (ζ) of the freshly prepared nanoparticles were measured by dynamic light scattering using a Zetasizer (Nano ZS, Malvern Instruments, Groveswood, UK). In particular, the nanoparticle suspension was diluted 10-fold with Milli-Q water for size and polydispersity index determination, while it was diluted 100-fold for zeta potential determination. All the measurements were performed in triplicate and the results are expressed as mean value \pm standard deviation (SD).

The particle size was confirmed using a qNano size analyzer (iZON Sciences, Christchurch, New Zealand) with a nanopore 200 (iZON NP 200) and 200 nm calibration particles (CP 200). A buffer containing sodium chloride (NaCl), Tris (pH 8), EDTA, and Triton-X in deionized water was used as the electrolyte to suspend the NP samples and the calibration particles. Each recorded measurement was based on a minimum particle count of 500 particles and analyzed using IZON Control Suite software 3.3 (Izon Science, Oxford, UK).

2.4.2. Nanoparticle surface morphology

Surface morphology of the nanoparticles was evaluated using scanning electron microscope (SEM) (FEI, Helios G3 UC Dual beam

ThermoFisher scientific, Waltham, MA, USA). For sample preparation, 10 μ L of nanoparticles in suspension were deposited on a metal stub and, after drying, the sample was coated with gold under vacuum for 120 s. The SEM images were analyzed using the free software ImageJ to determine the particles size.

2.4.3. Drug loading and entrapment efficiency

The drug loading of SV7 in the NPs was assayed by dissolving 100 μ L of SV7-loaded PLGA nanoparticles in 500 μ L of DCM and then following the RP-HPLC analytical procedure described above. The drug loading is reported as the percent of the amount of SV7 in relation to 10 mL of NP suspension \pm SD of the values collected from three different batches. The entrapment efficiency (EE) is reported as percentage of the ratio between the experimentally determined drug loading and the theoretic loading \pm SD of the values collected from three different batches.

2.4.4. Residual organic solvent after nanoparticles production

At the end of the NPs preparation, the residual content of organic solvents in the formulation was evaluated through static headspace gas chromatography–mass spectrometry (HS-GC–MS) (Müller et al. 2019). An Agilent Technologies 7890B gas chromatograph (Waldbronn, Germany) with an autosampler, PAL RSI 85 (CTC Analytics, Zwingen, Switzerland) was coupled with an Agilent Technologies 7010B triple quadrupole detector. The MS was operated in scan mode (m/z 50–150; EI 70 eV). An Agilent J&W GC column DB-624 Ultra Inert (6% cyanopropyl phenyl and 94% polydimethylsiloxane) 30 m \times 0.25 mm \times 1.4 μ m from Agilent Technologies (Waldbronn, Germany) was used as stationary phase. The carrier gas used was helium 99.999% from Air Liquide (Düsseldorf, Germany). The conditions of the headspace sampler and the GC–MS system are summarized in Supplementary Table 1. Of each sample, 100 mg were weighted into a 20 mL headspace vial, 5 mL deionized water, 2 g NaCl and 10 μ L of stable isotope-labeled internal standard solution (100 μ g/mL acetone- d_6 , SIL-IS) was added, and the vial was closed tightly. After sealing, the sample was analyzed by static HS-GC–MS. The molecule peaks of acetone and acetone- d_6 (SIL-IS) (m/z 58.1 and 64.2) were used as qualifier ions and the base peaks m/z 43.2 and 46.2 as quantifier ions.

2.4.5. Nano-embedded dry powder production through freeze-drying

Nano-embedded dry powders were produced through freeze-drying. The optimized SV7-loaded PLGA nanoparticles were shock frozen in liquid nitrogen and lyophilized overnight using a VirTis BenchTop Pro freeze dryer (SP Scientific, Warminster, PA, USA). To improve the dry powder properties after freeze-drying, different cryoprotectants, such as mannitol, trehalose and 2-hydroxypropyl- β -cyclodextrin (HP- β -CD), in different concentrations were tested. The dry powders were then stored in closed vials at room temperature in a desiccator. To evaluate the redispersibility of the freeze-dried powder, particle size analysis of the reconstituted liquid dispersion was performed through dynamic light scattering using a Zetasizer (Nano ZS, Malvern Instruments, Groveswood, UK), and the results are expressed as mean value \pm SD of value collected from three different batches.

2.4.6. In vitro release profile

The *in vitro* drug release behavior of SV7 from SV7-loaded PLGA nanoparticles, before and after freeze drying, was determined. Phosphate-buffered saline (PBS) (120 mM NaCl, 2.7 mM KCl, 10 mM Na₂HPO₄) at pH 7.2 with 0.2% Tween 80 was used as dissolution medium [26]. During the study, the samples were incubated at 37 °C with shaking. At scheduled time intervals, samples were centrifuged at 15,700 g for 10 min at 4 °C to isolate the NPs while the release medium was withdrawn and analyzed by UV spectroscopy for SV7 content as described above. The medium was replaced by the same amount of fresh PBS at pH 7.2. Experiments were carried out in triplicate and results expressed as cumulative release of SV7 from NPs \pm SD.

2.5. *In vitro* antimicrobial activity

The minimum inhibitory concentration (MIC) of SV7 as free compound and after encapsulation in PLGA NPs was determined by the broth microdilution method in 96-well microplates. Both gram-positive and gram-negative strains were used for the experiments: Methicillin sensitive *Staphylococcus aureus* (ATCC 29213), Methicillin resistant *Staphylococcus aureus* (ATCC 43300), *Pseudomonas aeruginosa* (ATCC 10145), *Escherichia coli* (ATCC 25922), *Klebsiella pneumoniae* (ATCC 700603) as well as *Pseudomonas aeruginosa*, *Enterobacter cloacae*, *Serratia marcescens*, *Klebsiella oxytoca*, *Citrobacter freundii*, and *Proteus vulgaris* from clinical isolates. Briefly, every strain was grown in Luria Bertani (LB) broth at 37 °C. The bacterial suspension to be used as the inoculum was diluted to yield an optical density (OD) around 0.5 at 600 nm (corresponding to about 1×10^9 CFU/mL). Afterwards, the bacterial cell suspension was further diluted 100-fold to produce a bacterial cell suspension of 10×10^4 CFU/mL. SV7 encapsulating PLGA nanoparticles were serially diluted 2-fold in Brain Heart Infusion (BHI) broth to achieve final concentrations ranging from 50 µg/mL to 0.1 µg/mL in a final volume of 200 µL (including 100 µL of bacterial suspension). Free SV7, ciprofloxacin, tobramycin and erythromycin (Amdipharm) were used as controls in the same concentration range used for SV7 encapsulating PLGA NPs. The bacterial suspension alone was used as the positive control, while the negative controls were the antibiotics at the highest concentrations and BHI broth alone. After 24 h of incubation, the plates were visually inspected. The MIC is defined as the lowest concentration of the tested antibiotic at which no growth of the inoculum was observed.

2.6. *In vitro* cytotoxicity on lung cells

2.6.1. Cell culture

Human adenocarcinoma alveolar based lung cancer cells (A549) were cultured in RPMI 1640 cell culture medium and supplemented with 1% penicillin/streptomycin and 10% fetal bovine serum (FBS). Human epithelial bronchial cells (16HBE14o-) were cultured in EMEM cell culture medium supplemented with 1% L-glutamine, 1% penicillin/streptomycin and 10% FBS. Cells were grown in 75 cm² cell culture flasks and passaged every 3 days with 0.05% and 0.25% trypsin, respectively. Cells were maintained in a humidified atmosphere at 37 °C and 5% CO₂.

2.6.2. Cell viability and lactate dehydrogenase (LDH) release

When confluent, A549 and 16HBE14o- cells were trypsinized and seeded at a density of 10,000 cells per well in 100 µL of medium in 96-well plates. Twenty-four hours after seeding, the medium was removed, and 100 µL of fresh medium containing different amounts of PLGA nanoparticles prepared with 2.5 mg SV7 (PLGA_2.5SV7) corresponding to a certain amount of SV7 entrapped (1.6, 8, 16, 40, 80 and 160 µg/mL of SV7), or their corresponding controls were added to each well. After the NP addition, the plates were incubated for 24 h, 48 h and 72 h respectively at 37 °C and 5% CO₂. At each time point, the medium from the wells was collected to assess the LDH release, after which 100 µL of a 0.5 mg/mL MTT sterile solution were added to each well. After 3 h of incubation, each well was washed with PBS and then 200 µL of a mixture of isopropanol and hydrochloric acid (0.04 M HCl in absolute isopropanol) were added and incubated on an orbital shaker for 15 min. The absorbance was read at 570 nm using a microplate reader (FLUOstar Omega, BMG Labtech). Control groups included cells treated with blank nanoparticles and free SV7 dissolved in DMSO. The percentage of viable cells was calculated by the ratio of absorbance of treated cells compared with untreated cells. Results are given as mean values of triplicates ± SEM.

CytoTox 96® non-Radioactive Cytotoxicity Assay (Promega, Madison, WI, USA) according to the manufacturer's guidelines was used to quantify the LDH release. The absorbance was read at 490 nm using a microplate reader (FLUOstar Omega, BMG Labtech). Control groups

included cells treated with blank nanoparticles. The percentage of cytotoxicity was calculated by the ratio of absorbance of treated cells compared with fully lysed cells (maximum LDH release control). Results are given as mean values of triplicates ± SEM.

2.7. *In vitro* cellular uptake

2.7.1. Cell culture

Mouse BALB/c monocyte macrophages (J774A.1) were cultured in DMEM cell culture medium supplemented with 1% glutamine, 1% penicillin/streptomycin and 10% FBS. Cells were grown in 75 cm² cell culture flasks at 37 °C and 5% CO₂.

2.7.2. Cellular uptake by flow cytometry

To evaluate the cellular uptake of nanoparticles by macrophages, the fluorescent dye coumarin-6 was incorporated in the SV7-PLGA formulation. J774A.1 macrophages were seeded at a density of 50,000 cells/well in a 24-well-plate and incubated for 24 h at 37 °C and 5% CO₂. Cells were then transfected with 100 µL of coumarin-6-loaded PLGA (PLGA_C6) nanoparticles suspension for 2, 4, 24 and 48 h. At different time points, cells were harvested and washed two times at 400 g for 5 min and resuspended in PBS/2 mM EDTA. Cells were analyzed using an Attune NxT flow cytometer (ThermoFisher Scientific, MA, USA) with 488 nm excitation and 530 nm emission filter. Cells were gated based on morphology resulting from forward/sideward scattering and 10,000 events were analyzed per sample. Results are given as mean values of triplicates ± SEM.

2.7.3. Confocal microscopy

J774A.1 macrophages were seeded in a 24-well-plate containing a cover glass at a density of 50,000 cells/well in 500 µL of medium and incubated for 24 h at 37 °C and 5% CO₂. The day after, cells were transfected with 100 µL of coumarin-6 loaded nanoparticles and incubated for 2, 4, 24 and 48 h. One hour before the incubation time was completed, cells were washed with PBS twice and incubated with 300 µL of a 75 nM LysoTracker® red (ThermoFisher Scientific, MA, USA) solution, an organelle-specific labeling dye. Cells were then washed twice with PBS and fixed with 4% paraformaldehyde for 15 min. After three washing steps, cells were finally incubated with DAPI (4',6-diamidino-2-phenylindole) at a final concentration of 1 µg/mL for 20 min. Cells were then washed twice again and mounted using FluorSave™ (Merck Millipore, Billerica, MA, USA) reagent for fluorescence microscopy. Fluorescent images were acquired using a SP8 inverted scanning confocal microscope (Leica Camera, Wetzlar, Germany).

2.8. SV7-loaded nanoparticles against MRSA intracellular infection

To evaluate the activity of SV7-loaded NPs against intracellular infections, J774A.1 macrophages were seeded in a 24-well-plate at a density of 50,000 cells/well in 500 µL of medium and incubated for 24 h at 37 °C and 5% CO₂. Afterwards, MRSA was added to the cells at a concentration of 2.5×10^5 CFU/well and co-cultivated for 1 h. Cells were then washed with PBS, and the medium was replaced with fresh medium containing 1 µg/mL gentamicin to remove extracellular MRSA. After 30 min, plates were washed with PBS and fresh medium containing free SV7 in DMSO, SV7-loaded NPs and empty NPs was added at final SV7 concentrations of 8.5, 17, 42.5 and 85 µg/mL. After 24 h, cells were lysed with ice-cold 0.1% Triton-X for 15 min and collected in microcentrifuge tubes. The lysates were serially diluted in PBS for colony count in blood agar plates. Bacterial colonies were counted after overnight incubation at 37 °C. The results are expressed as x-fold reduction in comparison to the cells that received only MRSA infection and no treatment.

2.9. In vivo antimicrobial activity

2.9.1. In vivo toxicity and survival of *Galleria mellonella* larvae

The antimicrobial activity of SV7-loaded nanoparticles was tested *in vivo* in the TruLarv™ *Galleria mellonella* (Biosystems Technology, Exeter, UK) model. The safety of the formulation was evaluated by injecting larvae with 10 μ L of the different samples (8.5 μ g/mL), and the survival percentage was observed for the following 96 h.

In a pre-treatment study, larvae received a 10 μ L injection of SV7-

loaded NPs or the respective unloaded control (8.5 μ g PLGA/mL), 24 h before the infection with LD₅₀ *S. aureus* methicillin-sensitive (2.5×10^5 CFU/mL) or *S. aureus* methicillin-resistant (7.5×10^5 CFU/mL). The LD₅₀ bacterial dose was experimentally determined for each strain in the *Galleria mellonella* model (Supplementary Fig. 1). Larvae were incubated in the dark at 37 °C and the survival percentage was monitored 24, 48 and 72 h post-infection. Each experiment consisted of 10 larvae per group. Control groups consisted of untreated larvae, PBS-only injected larvae, DMSO-only larvae, DMSO-SV7 larvae and infected-only larvae.

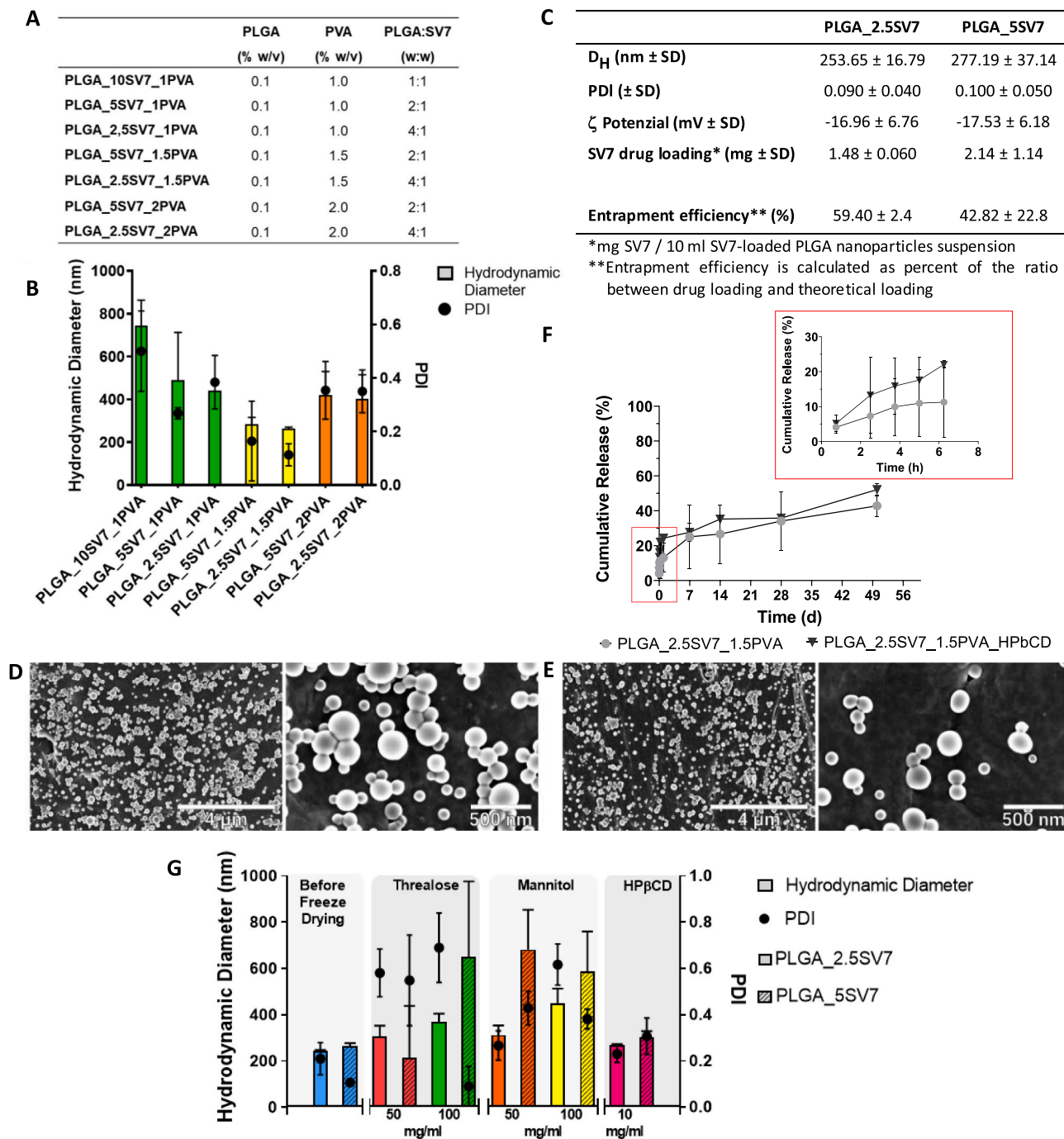


Fig. 1. SV7-loaded PLGA nanoparticles composition (A) and hydrodynamic diameter (D_H) (B) and polydispersity index (PDI) characterized by dynamic light scattering. (C) Overall characterization of PLGA_2.5SV7 and PLGA_5SV7. SEM images of (D) PLGA_5SV7 and PLGA_2.5SV7 (E); Scale bars represent 4 μ m and 500 nm for low magnification and high magnification images, respectively. (F) Release profile of PLGA_2.5SV7 NPs and PLGA_2.5SV7_ HP β CD NPs. (G) Hydrodynamic diameter and polydispersity index of PLGA_2.5SV7 and PLGA_5SV7 NPs reconstituted in water after lyophilization.

2.9.2. *Galleria mellonella* bleeding for residual bacterial load

In a following study, the residual bacterial load from larvae was evaluated by harvesting the haemolymph of 3 larvae per group (untreated, infected-only, PLGA NPs and SV7-PLGA NPs) 72 h post-infection. The haemolymph was serially diluted in PBS, and 15 μ L of each sample were plated on blood agar. Bacterial colonies were counted after overnight incubation at 37 °C.

2.9.3. 2.9.3 Statistical analysis

Percent survival of *G. mellonella* *in vivo* study was shown as Kaplan-Meier plots and statistical significance was determined using the log-rank (Mantel-Cox) test (GraphPad Prism 5.0). Statistical significance of the residual bacterial load in *G. mellonella* was analyzed by One-way ANOVA with Turkey post-test (GraphPad Prism 5.0). Statistical significance values were indicated as * $P < 0.05$, ** $P < 0.01$, *** $P < 0.005$.

3. Results and discussion

3.1. Production and characterization of SV7-loaded PLGA nanoparticles

SV7 is a novel benzophenone-based membrane-targeting antibiotic which is able to release potassium ions resulting in the disruption of the bacterial membrane. The major obstacle for its clinical application is its low aqueous solubility that can affect its dissolution in physiological fluid such as the lung lining fluid where bacteria causing pulmonary infections are located. Thus, SV7-loaded PLGA nanoparticles were prepared through a single evaporation emulsification method in order to encapsulate and deliver SV7, an approach previously exploited for controlled release purposes [25,27]. With special regard to SV7, in order to increase the reported encapsulation efficiency (EE) of 33.3 \pm 5.1%, an in-depth formulation study was carried out [25]. At first the best ratio between PLGA and a fixed amount of PVA was evaluated; Smaller NPs than previously reported were fabricated using a PLGA:PVA ratio equal to 0.1% w/v. (Supplementary Fig. 2). Then SV7 was added to the formulation varying parameters such as the surfactant concentration or the amount of payload added to the formulation (Fig. 1A). Through this approach, we determined that at the PLGA:SV7 ratio of 4:1 (PLGA_2.5SV7) and 2:1 (PLGA_5SV7), in presence of 1.5% w/v of PVA, NPs with a hydrodynamic diameter around 250 nm are obtained, which are suitable for lung administration (Ungaro et al. 2012; Sanders et al. 2000; Lim et al. 2016) (Fig. 1B).

In particular, the NP suspensions analyzed through Dynamic Light Scattering (DLS) showed dimensions of 277.2 \pm 37.1 and 253.7 \pm 16.8 nm, respectively, for PLGA_2.5SV7 and PLGA_5SV7 (Fig. 1C). The NP suspensions are of very homogenous nature with a polydispersity index (PDI) of 0.100 \pm 0.050 and 0.090 \pm 0.040 (Table 1C). Both formulations presented a negative ζ -potential around -17 mV (Table 1C).

A further in-depth particle diameter measurement was performed by tunable resistive pulse sensing (TRPS) (Kozak et al. 2012; Kozak et al. 2011; Hartl et al. 2019). In this case, the collected data displayed an

Table 1

Minimum inhibitory concentration of SV7, SV7-loaded NPs, ciprofloxacin, tobramycin and erythromycin against MSSA, MRSA and *P. aeruginosa*.

	MINIMUM INHIBITORY CONCENTRATION (MIC) (mg/L)		
	MSSA	MRSA	<i>P. aeruginosa</i>
Ciprofloxacin (Break point)*	0.7 (S \leq 1)	1.7 (S \leq 1)	0.2 (S \leq 0.5)
Tobramycin (Break point)*	n.d.**	n.d.**	0.4 (S \leq 4)
Erythromycin (Break point)*	n.d.**	n.d.**	(-)
SV7	1.7	1.8	n.d.**
PLGA_2.5SV7	9.4	12.5	n.d.**

* Break point reported by the “The European Committee on Antimicrobial Susceptibility Testing”. Breakpoint tables for interpretation of MICs and zone diameters. Version 8.1, 2018. <http://www.eucast.org>

** n.d.: no effect detected in the concentration range tested (100 and 0.05 mg/L).

even smaller mean diameter of 188 \pm 65 nm supported by a nanoparticle size distribution that shows how the majority of the particles population has a size lower than 250 nm (Supplementary Fig. 3). This difference can be attributed to the difference in the working principle between DLS and TRPS techniques, measuring hydrodynamic diameters and particles sizes, respectively. In fact, TRPS performing a particle-by-particle-measurement, can provide a high-resolution measurement which was confirmed through SEM observation. SEM images show particles with spherical shape and a size of 142.06 \pm 7.93 (Fig. 1D, Fig. 1E) as verified with manual size counting through image J [28].

Considering the major localization of MRSA in the respiratory tract, the ability of the SV7-loaded PLGA NPs to penetrate through the mucus barrier and reach the target is a key requirement. However, the mucus meshes operate through a “size-filtering” mechanism to stop diffusion of particles, and to successfully penetrate it a specific geometrical size is required (i.e.~ 200 nm) [19]. Overall, both formulations show promising features for penetrating the mucus barrier and reaching the bacteria. However, the particle geometry alone is not able to guarantee that ability of the formulation to deposit in the airways. The particle mass median aerodynamic diameter (MMAD), resulting from size, density and shape of the particle, critically influences the mechanism and the site of NPs deposition when delivered via the inhalation route. Thus, initial studies were carried out and confirmed the potential of the developed formulation to be used for local pulmonary administration through evaluation of the particle mass median aerodynamic diameter (MMAD) and in term of stability during the nebulization (Supplementary Fig. 4).

Finally, the freshly prepared SV7-loaded PLGA nanoparticles produced with 2.5 and 5 mg of SV7, respectively, were characterized also for their encapsulation efficiency (EE) (Fig. 1C).

EE is calculated as the ratio between the actual and the theoretical loading \times 100% and resulted in 59.4 \pm 2.4% and 42.8 \pm 22.8%, respectively, corresponding to a bulk loading of 1.48 \pm 0.060 and 2.14 \pm 1.14 mg of SV7 for batch. These results are considerably improved compared with the first report in which the EE was 33.3 \pm 5.13% [25]. Based on the higher entrapment efficiency, the formulation PLGA_2.5SV7 was selected for further characterization.

Considering that the production of PLGA_2.5SV7 nanoparticles involved a single evaporation emulsification method, a residual content of organic solvents could be found in the final NP suspensions. Because of the potential risk for the human health, the acceptable amount of residual solvent is strictly regulated by the authorities. Acetone is classified in class 3 which includes solvents considered less toxic and of lower risk. Nevertheless, the European medicines agency accepts, without further justification, residual solvents amount of 50 mg per day or less (corresponding to 5000 ppm or 0.5%) (Ph.Eur. 11th Ed.). To evaluate if the formulation responds to this required standard, the residual acetone was quantified through gas chromatography–mass spectrometry after nanoparticle production. The mean residual content of acetone was 0.45 μ g per 100 mg sample (w/w) corresponding to 0.0005% \pm 0.0001% (\pm SD, $n = 3$) assuring the tolerability of the formulation.

After production, the NP suspension was stored at 4 °C to test the stability over time (Supplementary Fig. 5). After 60 days of storage, almost a 0.5-fold increase in the particle hydrodynamic diameter was observed compared to the original value, while in the same time frame, the PDI showed a 4-fold increase. This instability is not surprising and is caused by hydrolytic degradation of PLGA in the aqueous environment, as well as the aggregation phenomena arising from its storage (De Jaeghere et al. 1999). However, in a translational perspective the need to extend the storage stability was highlighted. Thus, in order to enhance the shelf-life of the formulation and avoid the loss of native nanocarrier characteristics, a strategy commonly used by pharmaceutical industries with an easy industrial scale-up, namely lyophilization was used [29,30]. The optimized formulation PLGA_2.5SV7 was further processed to achieve a solid long-term stable lyophilized powder which can be reconstituted in saline solution. In order to prevent particles from

degrading and aggregating during freeze-drying, cryoprotectants were added to the NPs suspension. Excipients were preferred, which were already used for lung administration or that could add a functionality to the NPs suspension as airways rehydrating agents (i.e. mannitol, trehalose and 2-hydroxypropyl- β -cyclodextrin) [31].

The selected cryoprotectants were then added to the nanoparticle suspensions at different concentrations. After the solidification process, the hydrodynamic diameter and the polydispersity index of SV7-loaded PLGA NPs reconstituted through water addition after lyophilization was performed by dynamic light scattering analysis, and the results are reported in Fig. 1F.

The redispersibility index (RDI), defined as:

$$RDI = D/D_0$$

where D_0 represents the size of the nanoparticles prior to drying, and D represents the corresponding value post rehydration of the dried sample in water was calculated. A redispersibility index, whose value is as close as possible to 1 indicates that the powders obtained by lyophilization can be completely reconstituted in the initial formulation regarding size and PDI [32].

The best performance was obtained in presence of 100 mg/mL of HP β CD, which showed for PLGA_5SV7 a RDI of 1.15 and for PLGA_2.5SV7 a RDI of 1.10. Overall, considering the better performance of PLGA_2.5SV7, this formulation was selected for further experiments.

The ability of PLGA_2.5SV7 to release SV7 in physiological condition was evaluated showing a typical two-stage release profile (Fig. 1G). In particular, the freshly prepared PLGA_2.5SV7 NPs, after a burst effect in the first 6 h during which $11.3 \pm 2.6\%$ of the encapsulated SV7 was released, display a sustained release of the payload, lasting about 50 days and reach a final release of $42.7 \pm 6.0\%$ of the loaded drug. The release of SV7 was also evaluated after converting the NP suspensions into nano-embedded dry powders using HP β CD as cryoprotectant. The presence of HP β CD increased the rate and amount of SV7 released and causes a release of $22.1 \pm 1.1\%$ and $52.0 \pm 3.6\%$ respectively after 6 h and 50 days. This effect could be explained considering that CD offers many benefits, not only as cryoprotectant but also to improve the drug solubility of low-water soluble compounds such as SV7 [33–35]. The effect of HP β CD on the release was further highlighted by the fitting the release with the zero-order model equation, the first-order release model equation (Data not shown), the Higuchi model equation and the Korsmeyer-Peppas model equation (Supplementary Fig. 6) [36]. In fact, when HP β CD is not present in the formulation the release fit the Higuchi model (R^2 : 0.988), thus describing a diffusion process based on the Fick's law and dependent on the square root of time. When HP β CD is present in the formulation, the best correlation is seen with the Korsmeyer-Peppas model (R^2 : 0.891, R^2 : 0.984), highlighting the 2-stage release process and a release performance strongly affected by the presence of HP β CD (Supplementary Fig. 6).

3.2. *In vitro* antimicrobial activity

In order to evaluate if the encapsulation process caused a loss in efficacy of SV7, the inhibitory activity of SV7 after encapsulation in PLGA NPs was determined on methicillin-sensitive *Staphylococcus aureus* (MSSA), methicillin-resistant *Staphylococcus aureus* (MRSA), *Pseudomonas aeruginosa*, *Escherichia coli*, *Klebsiella pneumoniae*, as well as *Pseudomonas aeruginosa*, *Enterobacter cloacae*, *Serratia marcescens*, *Klebsiella oxytoca*, *Citrobacter freundii* and *Proteus vulgaris* from clinical isolates. Only the MIC collected on MSSA, MRSA and *P. aeruginosa* are reported in Table 1 while results are not shown for the other gram negative strains since, in the range of concentration tested, SV7 did not show any observable effect on the inoculum growth. For comparison, the MIC observed for conventional antibiotics (i.e. ciprofloxacin, tobramycin and erythromycin) and their break point from the “The European Committee on Antimicrobial Susceptibility Testing” are

reported (Breakpoint tables for interpretation of MICs and zone diameters. Version 8.1, 2018. <http://www.eucast.org>).

SV7 as free compound showed a MIC of 1.7 mg/L and 1.8 mg/L, respectively, against MSSA and MRSA. After encapsulation in the PLGA NPs, SV7 was able to exert its antimicrobial effect but with an increase in the MIC, specifically 9.4 mg/L for MSSA and 12.5 mg/L for MRSA. This indicated that the potency of SV7 had been adversely affected by the formulation process or could also be related to the slow release of SV7 from the NPs. At equivalent NP polymer concentrations examined, blank NPs had no discernible effects on the visible growth of the bacteria.

3.3. *In vitro* cytotoxicity on lung cells

3.3.1.1. Cell viability and LDH release. The effect of SV7-loaded PLGA NPs on cell viability was evaluated through the 3-(4,5-dimethylthiazol-2-yl)-2,5-diphenyltetrazolium bromide (MTT) and LDH release assays.

MTT assay is one of the common assays used to study cell viability and proliferation [37,38]. With this experiment, we aimed at evaluating the safety of our formulation at increasing concentrations of SV7 and over an extended time period. We tested the effect of PLGA_2.5SV7 NPs, the respective unloaded control and free SV7 dissolved in DMSO at different concentrations (1.6, 8, 16, 40, 80 and 160 μ g SV7/mL) on two different lung epithelial cell lines: A549 (Fig. 2A) and 16HBE140- (Fig. 2B). All concentrations tested are higher than the SV7 active concentration. Cell viability was monitored up to 72 h. As shown in Fig. 2, PLGA_2.5SV7 NPs showed a safe profile up to the highest concentrations tested, decreasing viability only at a concentration 100-fold higher than the MIC value at the longest exposure time. Moreover, this experiment confirms that encapsulation in PLGA NPs represents a valid strategy to improve biocompatibility and bioavailability [39]. In fact, the viability of cells treated with free SV7 dissolved in DMSO is much lower than SV7 encapsulated in PLGA NPs due to the toxic effect of the solvent on cells. This finding reinforces the value of PLGA-based nanoformulation as a tool for increasing biocompatibility and bioavailability of small molecules, in our case of a newly developed antibacterial agent.

The effect of different nanoparticle concentrations in terms of disruption of the cellular membrane was determined through the release of lactate dehydrogenase (LDH) in the cell supernatants [40]. The LDH release was tested in 16HBE140- cells after incubation with different NPs concentrations, corresponding to the MIC value, 10-fold and 100-fold MIC. In agreement to what was previously observed in the MTT assay, SV7-loaded NPs retained a safe profile at all concentrations and time points tested (Supplementary Fig. 6). Moreover, higher cytotoxicity was observed for free SV7 dissolved in DMSO, confirming the role of PLGA NPs as a safe and biocompatible delivery system.

3.4. *In vitro* cellular uptake

3.4.1. Cellular uptake by flow cytometry

Notably, there is a growing body of evidence demonstrating that *S. aureus* survives inside macrophages *in vitro* and *in vivo* [41], making it essential to target this intracellular population to clear infection. To evaluate if and for how long the NPs are internalized in J774A.1 murine macrophages were selected as common existing model for studying intracellular bacterial infection as a respiratory infection model [42–44]. The cellular uptake was determined by flow cytometry. Hence, PLGA NPs were loaded with Coumarin-6 (PLGA_C6), a fluorescent dye soluble in organic solvents and commonly used to evaluate cellular uptake of nanoparticles [27,45]. PLGA_C6 NPs retained the same properties of PLGA_SV7 NPs in terms of size and ζ -potential (Supplementary Table 2). Considering the extended-release profile of SV7_PLGA NPs, we investigated the uptake of Coumarin-6 loaded NPs at different time points (2, 4, 24 and 48 h). The median fluorescence intensity values

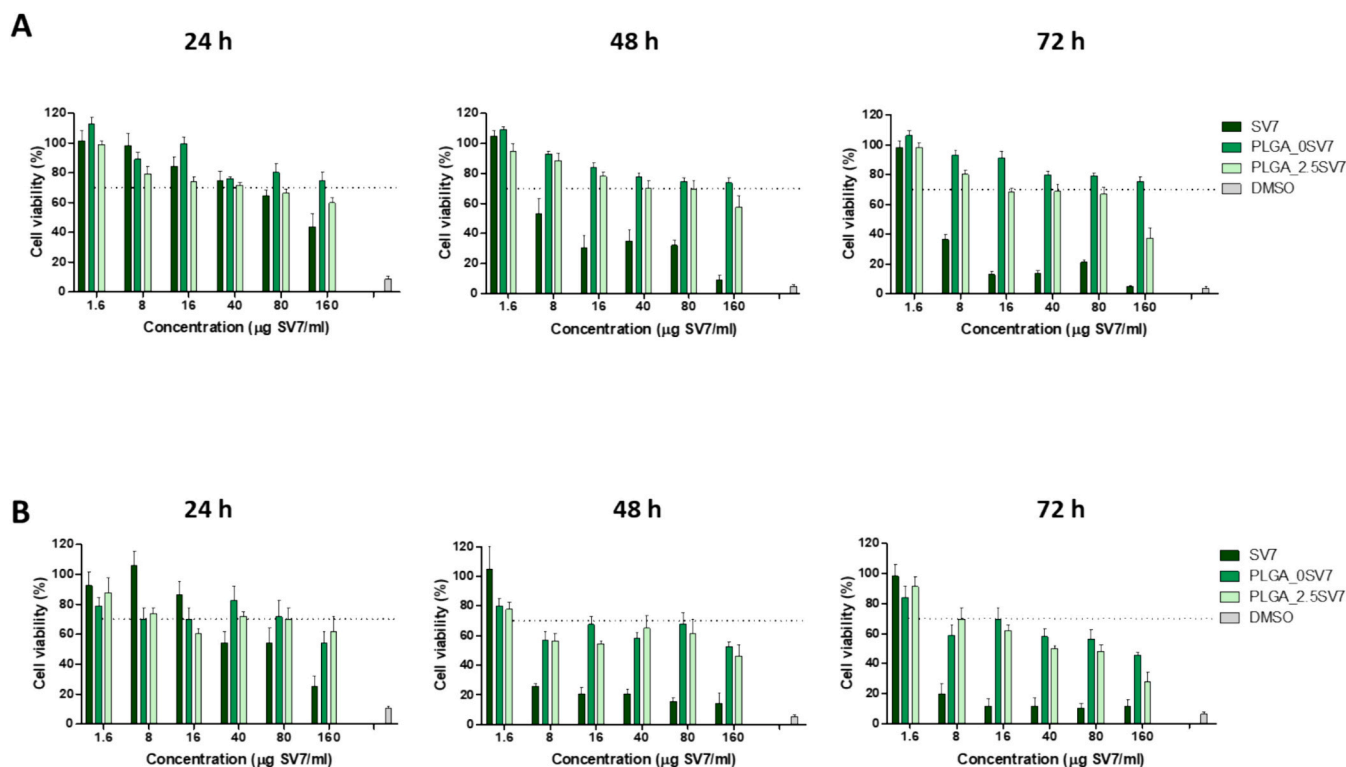


Fig. 2. Evaluation of cellular viability in A549 (A) and 16HBE14o- (B) cells after incubation with increasing amounts of PLGA_SV7 NPs and respective controls for 24, 48 and 72 h.

resulting from the flow cytometry analysis are presented in Fig. 3A. The results indicate that at each time point tested a significant uptake was observed in comparison to the respective untreated control group. Moreover, the uptake proved to be sustained over time, since the median fluorescence intensity values were comparable at all time points or slightly increased at longer time intervals. Additionally, this analysis also confirmed that the cellular uptake was homogenous in the cell population under investigation, since most of the cells were positively stained by coumarin-6 (data not shown). Our formulation retains optimal parameters for macrophage targeting. Nanoparticles in the size range of 200–500 nm, which are generally considered too big to be taken up by most cellular types, are indeed optimal to be recognized and phagocytosed by macrophages [46]. Our NPs, which have a hydrodynamic diameter of about 250 nm, well fit this observation and can be easily internalized by macrophages.

3.4.2. Confocal microscopy

To confirm the cellular internalization of PLGA_C6 NPs in J774A.1 macrophages, fluorescence images were acquired using an inverted scanning confocal microscope and the results are presented in Fig. 3B. In this experiment, nuclei were stained with DAPI (blue); lysosomes with LysoTracker® Red (red) and coumarin-6 is shown in green. At each time point tested, co-localization between the green fluorescence of coumarin-6 and the red fluorescence corresponding to the lysosomal staining can be observed. The overlap of the two fluorescence channels results in a yellowish color, confirming that the PLGA_C6 NPs were efficiently internalized by the macrophages and therefore represent a promising approach for the treatment of intracellular infections.

3.5. Inhibition of MRSA intracellular infection

After confirming the internalization of NPs by macrophages, the activity of the formulation against intracellular MRSA was investigated in a co-culture of J774A.1 macrophages and MRSA. After establishing

the co-culture, cells were treated with different concentrations of SV7-loaded NPs as well as empty NPs and free SV7 as controls. As shown in Fig. 4, SV7-loaded NPs retained about 50% of their activity against intracellular MRSA at the MIC for extracellular MRSA. This is not surprising as higher concentrations of antibiotics are generally required to eradicate intracellular infections [47]. Indeed, at a concentration 5 times the extracellular MIC, SV7-loaded NPs inhibited bacterial growth almost completely, therefore confirming the potential of the formulation as a valid ally against intracellular MRSA infections. Free SV7 showed higher activity against intracellular MRSA at a lower concentration than SV7-loaded NPs, in line with the results from the MIC study. This can be explained by the encapsulation of the antibiotic in the PLGA matrix, leading to longer times or higher concentrations required to achieve comparable concentration and activity as the free drug. Nonetheless, the encapsulation in PLGA NPs assures an improved safety profile of the formulation and a sustained release over time, which could be particularly important to prevent the establishment of intracellular infections in macrophages as well as decrease the risk of recurrent infection, while reducing the frequency of administration that could favor the development of antimicrobial resistance [48].

3.6. In vivo antimicrobial activity

The ability of free SV7 in DMSO to cure mice from lethal MRSA infection without inducing toxic effect has already been demonstrated [13]. However, SV7 as free compound, without a delivery system has little translational potential because of its low bioavailability. Therefore, after encapsulation of SV7, the efficacy of SV7-loaded NPs against *S. aureus* infections was examined *in vivo* in *G. mellonella* wax moth larvae, an established animal model used to provide an ethical and cost-effective proof of principle for novel antimicrobial agents [18,23,49–52]. Additionally, it also presents an innate response with many similarities to the human one as well as being able to survive at 37 °C. These properties make *G. mellonella* an ideal model for high

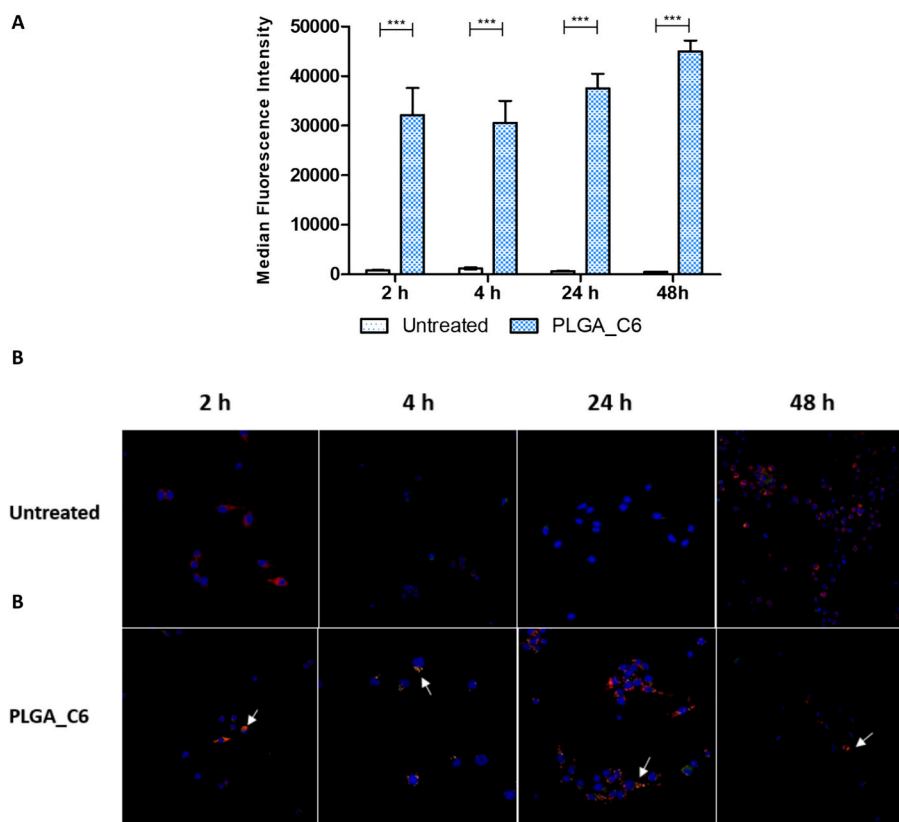


Fig. 3. (A) Cellular uptake of Coumarin-6 loaded NPs in J774A.1 murine macrophages measured by flow cytometry and presented as median fluorescence intensity \pm SD. Cells were analyzed after incubation with PLGA_C6 NPs for 2, 4, 24 and 48 h. Cellular uptake significance was measured using one-way ANOVA analysis in comparison to the untreated group. (B) Fluorescence microscopy of J774A.1 macrophages after transfection with PLGA_C6 NPs and staining with DAPI and Lyso-Tracker® Red at different time points with respective untreated controls. White arrows indicate co-localization between lysosome and PLGA_C6 NPs. (For interpretation of the references to color in this figure legend, the reader is referred to the web version of this article.)

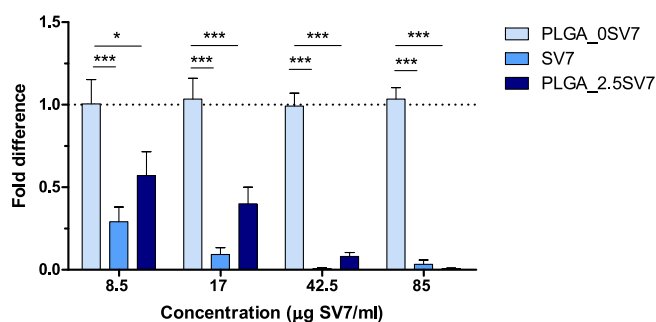


Fig. 4. Activity of SV7-loaded NPs against intracellular MRSA infection in J774A.1 macrophages. Statistical significance was calculated using One-Way ANOVA.

antimicrobial screenings, allowing a more accurate candidate selection for further studies [49].

3.6.1. Safety study

To investigate any potential toxic effect of the formulation, a safety study was conducted by injecting SV7-loaded NPs and the respective unloaded control in *G. mellonella* at the working concentration of 8.5 $\mu\text{g/ml}$. The percentage of survived animals was observed over the following 96 h. The formulation underlined a safe profile, resulting in the survival of all the treated animals, showing the same profile as the control group treated with PBS (Fig. 5A).

3.6.2. Pre-treatment study

Based on the controlled release nature of the formulation, a prophylactic treatment protocol was established to test the ability of SV7-loaded NPs to prevent the bacterial infection in *G. mellonella* and to extend the protection over time. In a preliminary experiment, in fact, it was observed that higher survival rates were achieved in the groups where NPs were administered before the bacterial infection in comparison to the groups receiving both injections at the same time (data not shown). Consequently, larvae were injected with LD₅₀ MSSA (2.5×10^5 CFU/mL), which was determined in a preliminary experiment (Supplementary Fig. 1), 24 h after the treatment with 8.5 $\mu\text{g/ml}$ SV7-loaded NPs, the respective unloaded NPs as control. The active concentration of SV7 in DMSO was determined in a preliminary experiment in which larvae were treated with increasing concentrations of SV7 in DMSO (Supplementary Fig. 1C). As it can be observed in Fig. 5B, SV7-loaded NPs mediated a significant improvement in the percentage of survived animals, with an increase of almost 40% in comparison to both the group, which received only the infection and the one treated with the unloaded NPs. Similar results were observed also for MRSA-infected larvae (Fig. 5C). In this case, SV7-loaded NPs allowed for the survival of 70% of the animals while without treatment the survival was only 30%.

3.6.3. *G. mellonella* bleeding for residual bacterial load

To confirm the results observed in the *in vivo* pre-treatment study, three larvae from each group were further analyzed for the residual bacterial load after 72 h from the infection as shown in Fig. 5 D, E. The results confirmed that the number of colonies detected for the group treated with SV7-loaded NPs was significantly decreased in comparison to both control groups that received only the infection with *S. aureus* or were treated with unloaded NPs.

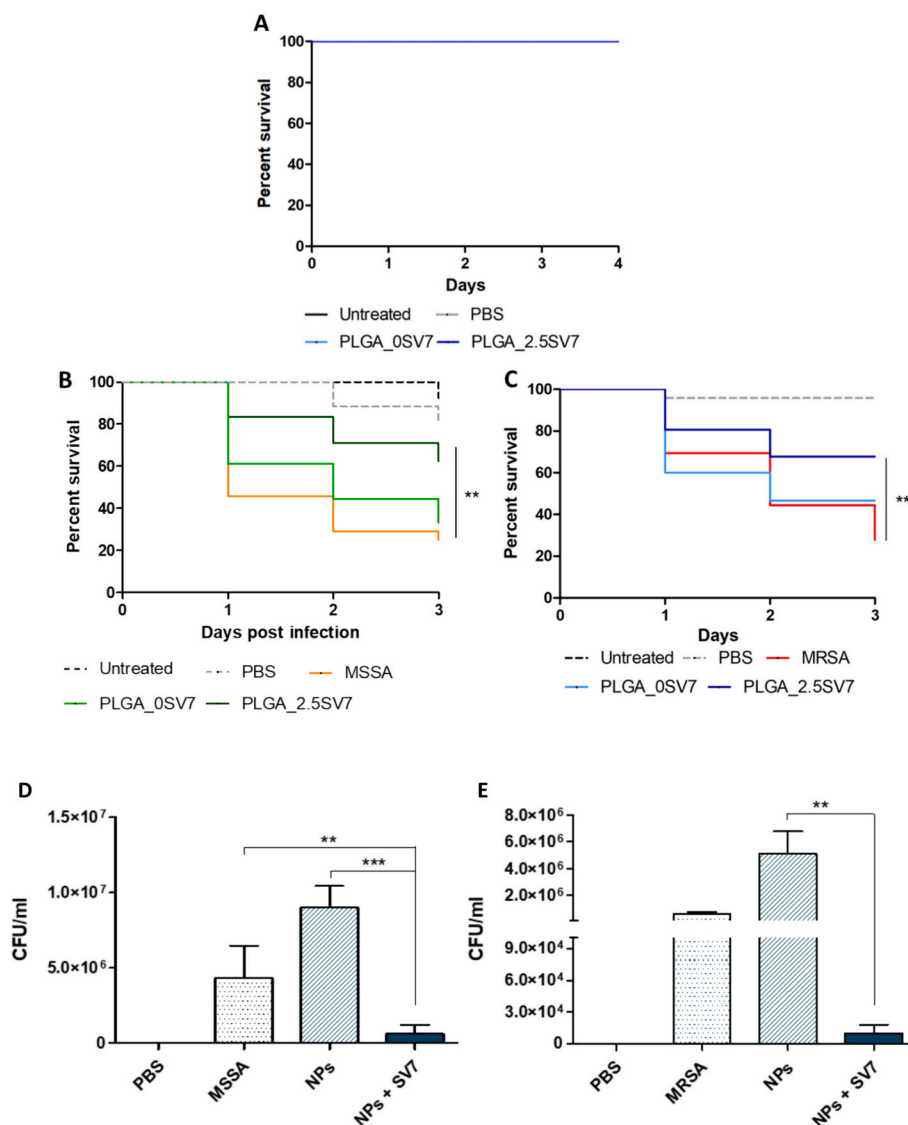


Fig. 5. Antibacterial activity and safety of SV7-loaded NPs in *G. mellonella* infection model. (A) PBS, PLGA NPs and PLGA_SV7 NPs were administered to uninfected larvae, and the survival was followed for the following 96 h. *G. mellonella* larvae were infected with MSSA (B) and MRSA (C) after 24 h pre-treatment with PLGA_SV7 NPs and the respective unloaded control. Percentage survival was monitored for the following 72 h. Statistical significance of survival was determined using the log-rank (Mantel-Cox) test. Residual bacterial load in *G. mellonella* was determined 72 h after the infection with MSSA (D) and MRSA (E). Bacterial load reduction was measured using One-Way ANOVA analysis of significance.

Similar observations were made also from the bleeding of MRSA-infected larvae. In this case, a consistent reduction of the residual bacterial load could be observed for the animals treated with SV7-loaded NPs in comparison to both control groups. Interestingly, both MSSA and MRSA-treated groups showed an increased bacterial load after the injection of unloaded PLGA NPs in comparison to the group that received only the infection. This might be explained due to the acidification of the environment following the degradation of PLGA NPs, which might have favored bacterial growth [53]. *S. aureus*, in fact, has an optimal growth at slightly acidic pH. However, animals treated with SV7-loaded NPs showed a marked reduction of bacterial load in comparison to both control groups. This experiment confirmed that PLGA_SV7 NPs prevent the establishment of *S. aureus* methicillin sensitive as well as *S. aureus* methicillin resistant infection in *G. mellonella*, supporting the observations suggesting that the antimicrobial agent retains its activity after the encapsulation in PLGA nanoparticles. Moreover, thanks to the sustained release profile of the formulation, the protection against infection could be retained over time.

4. Conclusion

In this study, we demonstrate the design and the development of a formulation approach that can enable the therapeutic activity of SV7, a novel benzophenone antibiotic, that otherwise cannot feasibly be used *in vivo* due to its poor water solubility. Therefore, we have focused on the production of PLGA_SV7 NPs which has been fully characterized for dimension, morphology, ability to mediate the sustained release of the payload and deposit in the deep airways for potential administration *via* inhalation. The safety of the formulation was demonstrated *in vitro* in lung cell lines and *in vivo* in the *G. mellonella* model. The efficacy against methicillin sensitive *S. aureus* (MSSA) and methicillin resistant *S. aureus* (MRSA) strains was demonstrated respectively *in vitro* in several bacteria strains and *in vivo* in the *G. mellonella* model. We further showed the ability of the NPs to be efficiently internalized by macrophages to target intracellular MRSA infection, which represents one of the biggest hurdles in the fight against being limited by the bacterial resistance process. Finally, to confirm the translatability of the findings, an *in vivo* *G. mellonella* infection model was established. Here, the safety of the

formulation as well as the activity of SV7-loaded NPs against MRSA in a prophylactic setup were confirmed. The pre-treatment with NPs in fact prevented the establishment of the infection and assured higher survival rates than control groups.

Overall, the results support the use of nanoformulation systems for the clearance of intracellular pulmonary infection that through local administration could avoid triggering of antimicrobial resistance. To exploit the advantageous findings of the NPs developed here, further studies are needed. For instance, optimization of the developed dry powder for delivery with a dry powder inhaler is very desirable and deserves further attention to enhance the patients' compliance to the therapy. Further *in vivo* studies in a more complex animal model (e.g. mice) will focus on the optimization of post-infection regimes, as well as in more complex environment such the effect on the tumor associated microbiome [7].

CRedit authorship contribution statement

Gabriella Costabile: Writing – original draft, Visualization, Methodology, Investigation, Funding acquisition, Formal analysis, Data curation, Conceptualization. **Domizia Baldassi:** Writing – original draft, Methodology, Investigation, Formal analysis, Data curation. **Christoph Müller:** Formal analysis. **Birgit Groß:** Methodology. **Francesca Ungaro:** Writing – review & editing, Funding acquisition, Conceptualization. **Sören Schubert:** Writing – review & editing, Supervision, Resources, Project administration, Methodology, Conceptualization. **Steven M. Firestine:** Writing – review & editing, Resources, Methodology, Funding acquisition. **Olivia M. Merkel:** Writing – review & editing, Supervision, Resources, Project administration, Funding acquisition, Conceptualization.

Declaration of competing interest

Olivia Merkel is a Scientific Board Member for Coriolis Pharma GmbH, AMW GmbH and Carver Biosciences and an Advisor for PARI Pharma GmbH, Boehringer-Ingelheim International GmbH, Cordem Pharma, and AbbVie Deutschland GmbH on unrelated projects.

Data availability

Data will be made available on request.

Acknowledgements

Olivia M. Merkel acknowledges Fondazione Ricerca Fibrosi Cistica, grant FFC#23/2017 and the European Research Council, grant ERC-2014-StG – 637830 for financial support.

Gabriella Costabile (GC) acknowledges UniNa and Compagnia San Paolo as recipient of a mobility fellowship in the frame of Programme STAR (CALL 2016) and Fondazione Umberto Veronesi for the post-doctoral fellowships (CALL 2019, CALL 2020) and sincerely thanks Dr. Thomas L. Moore for precious discussions and data analysis support.

Appendix A. Supplementary data

Supplementary data to this article can be found online at <https://doi.org/10.1016/j.jconrel.2024.08.029>.

References

- N.A. Turner, B.K. Sharma-Kuinkel, S.A. Maskarinec, E.M. Eichenberger, P.P. Shah, M. Carugati, et al., Methicillin-resistant *Staphylococcus aureus*: an overview of basic and clinical research, *Nat. Rev. Microbiol.* 17 (4) (2019 Apr) 203–218.
- R. Li, J. Li, X. Zhou, Lung microbiome: new insights into the pathogenesis of respiratory diseases, *Signal Transduct. Target Ther.* 9 (1) (2024) 19, <https://doi.org/10.1038/s41392-023-01722-y>. Available from: .
- J.B. Lyczak, C.L. Cannon, G.B. Pier, Lung infections associated with cystic fibrosis, *Clin. Microbiol. Rev.* 15 (2) (2002 Apr) 194–222.
- H.-X. Liu, L.-L. Tao, J. Zhang, Y.-G. Zhu, Y. Zheng, D. Liu, et al., Difference of lower airway microbiome in bilateral protected specimen brush between lung cancer patients with unilateral lobar masses and control subjects, *Int. J. Cancer* 142 (4) (2018 Feb) 769–778.
- C. Jin, G.K. Lagoudas, C. Zhao, S. Bullman, A. Bhutkar, B. Hu, et al., Commensal microbiota promote lung cancer development via $\gamma\delta$ T cells, *Cell* 176 (5) (2019 Feb) 998–1013.e16.
- L.M. Wong, N. Shende, W.T. Li, G. Castaneda, L. Apostol, E.Y. Chang, et al., Comparative analysis of age- and gender-associated microbiome in lung adenocarcinoma and lung squamous cell carcinoma, *Cancers (Basel)* 12 (6) (2020 Jun).
- M. Wang, B. Rousseau, K. Qiu, G. Huang, Y. Zhang, H. Su, et al., Killing tumor-associated bacteria with a liposomal antibiotic generates neoantigens that induce anti-tumor immune responses, *Nat. Biotechnol.* (2023), <https://doi.org/10.1038/s41587-023-01957-8>. Available from: .
- C. Garzoni, W.L. Kelley, *Staphylococcus aureus*: new evidence for intracellular persistence, *Trends Microbiol.* 17 (2) (2009 Feb) 59–65.
- M. Kubica, K. Guzik, J. Koziel, M. Zarebski, W. Richter, B. Gajkowska, et al., A potential new pathway for *Staphylococcus aureus* dissemination: the silent survival of *S. aureus* phagocytosed by human monocyte-derived macrophages, *PLoS One* 3 (1) (2008 Jan) e1409.
- X. Wang, X. Wang, D. Teng, R. Mao, Y. Hao, N. Yang, et al., Increased intracellular activity of MP1102 and NZ2114 against *Staphylococcus aureus* in vitro and in vivo, *Sci. Rep.* 8 (1) (2018 Mar) 4204.
- J. Braverman, I.R. Monk, C. Ge, G.P. Westall, T.P. Stinear, L.M. Wakim, *Staphylococcus aureus* specific lung resident memory CD4(+) Th1 cells attenuate the severity of influenza virus induced secondary bacterial pneumonia, *Mucosal Immunol.* 15 (4) (2022 Apr) 783–796.
- S.K. Vooturi, C.M. Cheung, M.J. Rybak, S.M. Firestine, Design, synthesis, and structure-activity relationships of benzophenone-based tetraamides as novel antibacterial agents, *J. Med. Chem.* 52 (16) (2009 Aug) 5020–5031.
- S.K. Vooturi, S.M. Firestine, Solution-phase parallel synthesis of novel membrane-targeted antibiotics, *J. Comb. Chem.* 12 (1) (2010) 151–160.
- S.K. Vooturi, M.B. Dewal, S.M. Firestine, Examination of a synthetic benzophenone membrane-targeted antibiotic, *Org. Biomol. Chem.* 9 (18) (2011 Sep) 6367–6372.
- N. Abed, P. Couvreur, Nanocarriers for antibiotics: a promising solution to treat intracellular bacterial infections, *Int. J. Antimicrob. Agents* 43 (6) (2014 Jun) 485–496.
- M. Chen, J. He, S. Xie, T. Wang, P. Ran, Z. Zhang, et al., Intracellular bacteria destruction via traceable enzymes-responsive release and deferoxamine-mediated ingestion of antibiotics, *J. Control. Release* 322 (2020) 326–336. Available from: <https://www.sciencedirect.com/science/article/pii/S0168365920301899>.
- W.K. Lau, D. Dharmasena, H. Horsley, N.V. Jafari, J. Malone-Lee, E. Stride, et al., Novel antibiotic-loaded particles conferring eradication of deep tissue bacterial reservoirs for the treatment of chronic urinary tract infection, *J. Control. Release* 328 (2020) 490–502. Available from: <https://www.sciencedirect.com/science/article/pii/S0168365920304892>.
- L. Jiang, M.K. Greene, J.L. Insua, J.S. Pessoa, D.M. Small, P. Smyth, et al., Clearance of intracellular *Klebsiella pneumoniae* infection using gentamicin-loaded nanoparticles, *J. Control. Release* 279 (2018 Jun) 316–325.
- G. Costabile, G. Conte, S. Brusco, P. Savadi, A. Miro, F. Quaglia, et al., State-of-the-art review on inhalable lipid and polymer nanocarriers: design and development perspectives, *Pharmaceutics* 16 (3) (2024). Available from: <https://www.mdpi.com/1999-4923/16/3/347>.
- Q.T. Zhou, S.S.Y. Leung, P. Tang, T. Parumasivam, Z.H. Loh, H.-K. Chan, Inhaled formulations and pulmonary drug delivery systems for respiratory infections, *Adv. Drug Deliv. Rev.* 85 (2015 May) 83–99.
- Z. Liang, R. Ni, J. Zhou, S. Mao, Recent advances in controlled pulmonary drug delivery, *Drug Discov. Today* 20 (3) (2015 Mar) 380–389.
- Y.H. Lim, K.M. Tiemann, D.A. Hunstad, M. Elsbahy, K.L. Wooley, Polymeric nanoparticles in development for treatment of pulmonary infectious diseases, *Wiley Interdiscip. Rev. Nanomed. Nanobiotechnol.* 8 (6) (2016 Nov) 842–871.
- G. Costabile, R. Provenzano, A. Zazzali, V.C. Scoffone, L.R. Chiarelli, V. Rondelli, et al., PEGylated mucus-penetrating nanocrystals for lung delivery of a new FtsZ inhibitor against *Burkholderia cenocepacia* infection, *Nanomedicine* 23 (2020 Jan) 102113.
- M.A. Cutuli, G. Petronio Petronio, F. Vergalito, I. Magnifico, L. Pietrangelo, N. Venditti, et al., *Galleria mellonella* as a consolidated in vivo model hosts: new developments in antibacterial strategies and novel drug testing, *Virulence* 10 (1) (2019 Dec) 527–541.
- G. Costabile, K.I. Gasteyer, V. Nadithe, K. Van Denburgh, Q. Lin, S. Sharma, et al., Physicochemical and in vitro evaluation of drug delivery of an antibacterial synthetic benzophenone in biodegradable PLGA nanoparticles, *AAPS PharmSciTech* 19 (8) (2018 Nov) 3561–3570.
- N. Günday Türel, A. Torge, J. Juntke, B.C. Schwarz, N. Schneider-Daum, A. E. Türel, et al., Ciprofloxacin-loaded PLGA nanoparticles against cystic fibrosis *P. aeruginosa* lung infections, *Eur. J. Pharm. Biopharm.* 117 (2017 Aug) 363–371.
- M. Andima, G. Costabile, L. Isert, A.J. Ndakala, S. Derese, O.M. Merkel, Evaluation of β -Sitosterol loaded PLGA and PEG-PLA nanoparticles for effective treatment of breast cancer: preparation, physicochemical characterization, and antitumor activity, *Pharmaceutics* 10 (4) (2018 Nov).
- D. Kozak, W. Anderson, R. Vogel, M. Trau, Advances in resistive pulse sensors: devices bridging the void between molecular and microscopic detection, *Nano Today* 6 (5) (2011 Oct) 531–545.

- [29] F. Franks, Freeze-drying of bioproducts: putting principles into practice, *Eur. J. Pharm. Biopharm.* 45 (3) (1998 May) 221–229.
- [30] Y.N. Konan, R. Gurny, E. Allémann, Preparation and characterization of sterile and freeze-dried sub-200 nm nanoparticles, *Int. J. Pharm.* 233 (1–2) (2002 Feb) 239–252.
- [31] G. Pilcer, K. Amighi, Formulation strategy and use of excipients in pulmonary drug delivery, *Int. J. Pharm.* 392 (1–2) (2010 Jun) 1–19.
- [32] G. Costabile, I. d'Angelo, G. Rampioni, R. Bondi, B. Pompili, F. Ascenzioni, et al., Toward repositioning niclosamide for antivirulence therapy of *Pseudomonas aeruginosa* lung infections: development of inhalable formulations through nanosuspension technology, *Mol. Pharm.* 12 (8) (2015 Aug) 2604–2617.
- [33] T. Loftsson, M.E. Brewster, Cyclodextrins as functional excipients: methods to enhance complexation efficiency, *J. Pharm. Sci.* 101 (9) (2012 Sep) 3019–3032.
- [34] H. Shelley, R.J. Babu, Role of cyclodextrins in nanoparticle-based drug delivery systems, *J. Pharm. Sci.* 107 (7) (2018 Jul) 1741–1753.
- [35] F. Li, Y. Wen, Y. Zhang, K. Zheng, J. Ban, Q. Xie, et al., Characterisation of 2-HP- β -cyclodextrin-PLGA nanoparticle complexes for potential use as ocular drug delivery vehicles, *Artif Cells, Nanomed. Biotechnol.* 47 (1) (2019 Dec) 4097–4108.
- [36] 5 - mathematical models of drug release, in: M.L. Bruschi (Ed.), *Strategies to Modify the Drug Release from Pharmaceutical Systems*, 2015, pp. 63–86. Available from: <https://www.sciencedirect.com/science/article/pii/B9780081000922000059>.
- [37] F. Denizot, R. Lang, Rapid colorimetric assay for cell growth and survival. Modifications to the tetrazolium dye procedure giving improved sensitivity and reliability, *J. Immunol. Methods* 89 (2) (1986 May) 271–277.
- [38] T. Mosmann, Rapid colorimetric assay for cellular growth and survival: application to proliferation and cytotoxicity assays, *J. Immunol. Methods* 65 (1–2) (1983 Dec) 55–63.
- [39] E.M. Elmowafy, M. Tiboni, M.E. Soliman, Biocompatibility, biodegradation and biomedical applications of poly(lactic acid)/poly(lactic-co-glycolic acid) micro and nanoparticles, *J. Pharm. Investig.* 49 (2019) 347–380, <https://doi.org/10.1007/s40005-019-00439-x>. Available from:
- [40] P. Kumar, A. Nagarajan, P.D. Uchil, Analysis of cell viability by the lactate dehydrogenase assay, *Cold Spring Harb Protoc* 2018 (6) (2018 Jun).
- [41] R.S. Flannagan, D.E. Heinrichs, Macrophage-driven nutrient delivery to phagosomal *Staphylococcus aureus* supports bacterial growth, *EMBO Rep.* 21 (8) (2020 Aug) e50348.
- [42] Y. Pei, M.F. Mohamed, M.N. Seleem, Y. Yeo, Particle engineering for intracellular delivery of vancomycin to methicillin-resistant *Staphylococcus aureus* (MRSA)-infected macrophages, *J. Control. Release* 267 (2017) 133–143. Available from: <https://www.sciencedirect.com/science/article/pii/S0168365917307745>.
- [43] F. Peyrussou, A. Van Wesse, G. Dieppo, F. Van Bambeke, P.M. Tulkens, Cellular pharmacokinetics and intracellular activity of the bacterial fatty acid synthesis inhibitor, afabacin desphosphono against different resistance phenotypes of *Staphylococcus aureus* in models of cultured phagocytic cells, *Int. J. Antimicrob. Agents* 55 (2) (2020) 105848. Available from: <https://www.sciencedirect.com/science/article/pii/S092485791930319X>.
- [44] Y. Li, Y. Liu, Y. Ren, L. Su, A. Li, Y. An, et al., Coating of a novel antimicrobial nanoparticle with a macrophage membrane for the selective entry into infected macrophages and killing of intracellular staphylococci, *Adv. Funct. Mater.* 30 (48) (2020 Nov).
- [45] N. Bege, T. Renette, M. Jansch, R. Reul, O. Merkel, H. Petersen, et al., Biodegradable poly(ethylene carbonate) nanoparticles as a promising drug delivery system with “stealth” potential, *Macromol. Biosci.* 11 (7) (2011 Jul) 897–904.
- [46] T. Mosaiab, D.C. Farr, M.J. Kiefel, T.A. Houston, Carbohydrate-based nanocarriers and their application to target macrophages and deliver antimicrobial agents, *Adv. Drug Deliv. Rev.* 151–152 (2019) 94–129.
- [47] E. Imbuluzqueta, Drug delivery systems for potential treatment of intracellular bacterial infections, *Front. Biosci.* 15 (1) (2010) 397.
- [48] S. Subramaniam, P. Joyce, N. Thomas, C.A. Prestidge, Bioinspired drug delivery strategies for repurposing conventional antibiotics against intracellular infections, *Adv. Drug Deliv. Rev.* 177 (2021 Oct) 113948.
- [49] C.J.-Y. Tsai, J.M.S. Loh, T. Profit, *Galleria mellonella* infection models for the study of bacterial diseases and for antimicrobial drug testing, *Virulence* 7 (3) (2016 Apr) 214–229.
- [50] R.D. Herculano, C.E. dos Reis, S.M.B. de Souza, G.S. Pegorin Brasil, M. Scontri, S. Kawakita, et al., Amphotericin B-loaded natural latex dressing for treating *Candida albicans* wound infections using galleria mellonella model, *J. Control. Release* 365 (2024) 744–758. Available from: <https://www.sciencedirect.com/science/article/pii/S0168365923007940>.
- [51] J. Deacon, S.M. Abdelghany, D.J. Quinn, D. Schmid, J. Megaw, R.F. Donnelly, et al., Antimicrobial efficacy of tobramycin polymeric nanoparticles for *Pseudomonas aeruginosa* infections in cystic fibrosis: formulation, characterisation and functionalisation with dornase alfa (DNase), *J. Control. Release* 198 (Jan 2015) 55–61.
- [52] R.Y.K. Chang, S.C. Nang, H.-K. Chan, J. Li, Novel antimicrobial agents for combating antibiotic-resistant bacteria, *Adv. Drug Deliv. Rev.* 187 (2022) 114378. Available from: <https://www.sciencedirect.com/science/article/pii/S0169409X2200268X>.
- [53] A. Medveov, Valk ubomr., *Staphylococcus aureus*: characterisation and quantitative growth description in milk and artisanal raw milk cheese production, *Struct Funct. Food Eng.* June 2014 (2012).